ISIJ International, Vol. 49 (2009), No. 6, pp. 911–920

Austenite Recrystallization–Precipitation Interaction in Niobium Microalloyed Steels

Stephanie VERVYNCKT,[1)] Kim VERBEKEN,[1,2)] Philippe THIBAUX,[3)] Martin LIEBEHERR[3)] and Yvan HOUBAERT[1)]

1) Department of Materials Science and Engineering, Ghent University, Technologiepark 903, B-9052 Ghent, Belgium. E-mail: Stephanie.Vervynckt@UGent.be 2) Max-Planck-Institut für Eisenforschung, Max-Planck-Strasse 1, 40237 Düsseldorf, Germany. 3) OCAS N.V., ArcelorMittal R&D Industry Ghent, J. F. Kennedylaan 3, B-9060 Zelzate, Belgium.

(*Received on October 29, 2008; accepted on February 17, 2009*)

A good combination of strength and toughness in HSLA steels can be achieved by the addition of microalloying elements such as Nb. Nb can retard the static recrystallization of austenite at lower temperatures by solute drag or by precipitation pinning. In this study, the recrystallization behavior of four Nb-microalloyed model alloys which were designed to show either extensive or almost no precipitation, was compared by multi-hit torsion tests and double hit compression tests. A good consistency between the different types of tests was found and the results were verified by optical micrographs. Further, by construction of softening–time–temperature diagrams the recrystallization behavior was linked to the precipitation state of the material which was investigated by thermodynamical equilibrium calculations and by experimental observations from TEM-EDX, Inductively Coupled Plasma Mass Spectroscopy and X-ray Diffraction. Quantitative agreement between the experimental measurements and the calculations for precipitated mass fraction and precipitate composition as a function of temperature and steel composition is demonstrated.

KEY WORDS: recrystallization; microalloyed steels; precipitation; solute drag.

1. Introduction

The use of heavy gauge steel sheets for structural applications very often requires a combination of high yield strength and adequate toughness. The most cost effective way to realize a high yield strength and a high ductility in a low alloyed steel is grain refinement. In industrial practice, this refinement is commonly realized by thermomechanical controlled processing (TMCP). The process includes slab reheating under well defined temperatures, a high amount of hot deformation below the non-recrystallization temperature (T_{nr}) and accelerated cooling. The non-recrystallization temperature is defined as the temperature below which no complete static recrystallization occurs between two successive rolling passes. In practice, the grain refinement is achieved by the addition of microalloying elements such as Nb and Ti.[1)] The effect of Ti is more or less incontestable, *i.e.* the formation of TiN precipitates inhibits grain growth, whereas the role of Nb in retarding the austenite recrystallization in High Strength Low Alloy (HSLA) steels has been the subject of considerable interest and discussion over the past 30 years.[2–4)] Previous research[5,6)] suggests that the retardation of austenite recrystallization in Nb-containing steels results from the pinning of austenite grain boundaries and subboundaries by either niobium carbonitride precipitation and/or by niobium atoms in solid solution in austenite. Although previous investigations have provided valuable knowledge on the effect of precipitation on the recrystallization, it is presently not possible to distinguish well the effect of both mechanisms, *i.e.* solute drag and precipitation pinning. On the one hand, if the recrystallization kinetics would be controlled by solute drag, then it would only be necessary to consider the concentration of microalloying elements dissolved in the austenite matrix. On the other hand, if carbonitride precipitation controls the recrystallization kinetics, then the levels of carbon and nitrogen in solution would also be important. Speer and Hansen[3)] investigated the austenite recrystallization in Nb microalloyed steels, showing that the solute drag effects on the austenite recrystallization are very small compared to the effect of carbonitride precipitation. Nevertheless, other investigators argue strongly in favor of the solute drag effect (*e.g.* Coladas *et al.*[7)]) or of a combination of the both effects.[8,9)]

Thermodynamic analysis is known to be an important method for optimizing both the chemistry and process design of microalloyed steels for thermomechanical processing. So far there is relatively little experimental data on phase equilibriums of carbonitrides in commercial steels, which makes it difficult to examine the validity of the calculations with respect to experimental findings. It has already been illustrated by Inoue *et al.*[10)] that thermodynamic equilibrium analysis of precipitates is a promising tool. These authors found good agreement between their equilibrium calculations and experimental data on the precipitated weight fraction of (Nb, Ti, V)(C, N) precipitates in hot rolled microalloyed steels. Moreover, Zou and Kirkaldy[11)] showed quantitative agreement between equilibrium calculations and the experimentally determined stoichiometry of (Nb, Ti)(C, N) precipitates in a non-deformed material. So far, the present authors found no direct comparison between the calculated equilibrium mole fraction of elements in a precipitate and experimental observations of the stoichiometry of precipitates during or after hot deformation, except a recent publication by Liu[12)] who compared his calcula-

tions with experimental data from Craven *et al.*[13)]

The objective of the present paper is to separate both retarding mechanisms, *i.e.* solute drag and precipitation pinning, by investigating model alloys designed to show either extensive or almost no precipitation. Moreover, the recrystallization kinetics of four Nb-microalloyed steels during hot deformation is linked to the morphology and composition of the precipitates and the amount of Nb-solutes found in these materials. The recrystallization kinetics were investigated combining different hot deformation testing techniques while information on the precipitation state of the material was obtained from thermodynamic equilibrium calculations and from a combination of experimental observation techniques. With this work, a contribution to the understanding of the fundamental mechanisms responsible for the retardation of austenite recrystallization in Nb-microalloyed steels is achieved.

2. Experimental Procedure

Four model alloys were designed and casted as 100 kg ingots in a Pfeiffer vacuum furnace operated under argon gas atmosphere. The chemical composition of these alloys can be found in **Table 1**. The C–Mn-reference alloy, without additional Nb, represents a reference steel. The second alloy, a lowC–Mn–Nb alloy containing only a few ppm C, allowed to study the effect of Nb in solid solution. The third alloy (C–Mn–Nb) was designed to study the effect of NbC-precipitates on the recrystallization kinetics. To have the highest fraction of NbC precipitates possible, a stoichiometric Nb/C-ratio of 8/1 was chosen. Finally, the fourth alloy (C–Mn–Nb–N) was designed to study the influence of N on the recrystallization and precipitation behavior. The cast blocks were thermomechanically processed under conditions comparable to those during industrial steel plate rolling. This means that, after a reheating cycle of 2 h at 1 200°C, two pre-rolling steps with 20% of deformation each were given above 1 100°C. Before finish rolling, the plate was air cooled until a temperature of 900°C was reached. Finishing was performed in five passes with a total reduction of 55%. After finish rolling at 820°C, the plates were air cooled to room temperature.

Torsion test specimens were machined from the plates with the specimen long axis parallel to the transverse direction of the plate. The specimens had a gauge length of 25 mm and a gauge diameter of 6 mm. The torsion tests were performed under argon atmosphere on a computerized torsion machine equipped with an induction heating system. For T_{nr} determination, the torsion specimens were first reheated to 1 250°C for 5 min. Subsequently, the samples were subjected to a series of consecutive deformations (multiple hits, strain 0.3, strain rate 1/s) separated by 20 s intervals, while the specimen was cooled at 1°C/s.[1)] At least three specimens per grade were tested to ensure reproducibility of the results. For each of the deformation passes the torque and the angle of twist were measured and converted to Von Mises effective stresses s and strains ε.[14)]

The isothermal recrystallization kinetics were determined from double hit compression tests with various interpass times. For these tests, cylindrical samples with a diameter of 5 mm and a height of 10 mm were machined by spark-erosion; the axis of the sample being parallel to the normal direction of the plate. The specimens were tested under vacuum under uni-axial conditions in a Bähr®-dilatometer equipped with an induction coil and a deformation unit. After reheating for 5 min at 1 250°C (same conditions as used for the multideformation torsion tests) and subsequent cooling at a cooling rate of 1°C/s to a chosen deformation temperature, a first deformation pass with a strain of 0.2 and a strain rate of 0.5/s was given. After deformation, the stress was immediately relieved to a minimum value necessary to keep the sample in position. After different chosen waiting times, a second deformation pass (also with $\varepsilon=0.2$, $d\varepsilon/dt=0.5$/s) was applied. Subsequently, the samples were helium quenched and prepared for optical microscopy. The Béchet–Beaujard etchant was used to reveal the former austenite grain boundaries.

Table 1. Chemical composition of the steels (in wt% unless stated otherwise).

	C	Mn	Si	Al	Nb	Ti	N
C-Mn reference	0.02	1.50	0.26	0.043	-	20 ppm	18 ppm
lowC-Mn-Nb	11 ppm	1.47	0.26	0.022	0.17	40 ppm	12 ppm
C-Mn-Nb	0.02	1.5	0.26	0.067	0.17	80 ppm	20 ppm
C-Mn-Nb-N	0.02	1.48	0.26	0.033	0.18	45 ppm	66 ppm

For the thermodynamic analysis of the precipitates, the Thermocalc® package (database TCFE3) was used. The experimental precipitate composition and size distribution were determined on a 200 kV JEOL JEM-2200FS Transmission Electron Microscope (TEM) in combination with an Energy Dispersive X-ray Spectrometer (EDX), using carbon extraction replicas. The total amount of niobium precipitated was analyzed by Inductively Coupled Plasma Mass Spectrometry (ICP-MS). In these experiments, a small amount of material is selectively dissolved and the resulting solution is filtered through a 20 nm pore size filter. The filtrate contains the dissolved Fe-matrix together with the elements in solid solution, while the filter traps the insoluble precipitates. The weight fraction of Nb on the filter and in the filtrate was quantitatively determined. Furthermore, the stoichiometry of the precipitates was determined by performing X-Ray Diffraction (XRD) analysis on the filters. For the radiation a Cu-Kα source was used.

3. Characterization of the Recrystallization Behavior

3.1. Determination of the Non-recrystallization Temperature (T_{nr})

From the stress–strain curves obtained in a multideformation torsion test, the mean flow stress (MFS) corresponding to each pass can be calculated by numerical integration and plotted against the inverse of absolute temperature. The MFS is the area under each stress–strain curve divided by the pass strain. In **Fig. 1**, typical examples of the evolution of the mean flow stress (MFS) during multideformation testing are plotted. Two different regions can be clearly distinguished for all steels. In the high temperature region, full recrystallization takes place between two deformations and the increase in stress is solely due to the decrease in temperature. In the second region, which corresponds to deformation below T_{nr}, only partial recrystallization or no recrystallization occurs. Here, the strain is accumulated from pass to pass, so that the stress increases more rapidly with decreasing temperature. Following the method developed by Jonas and co-workers,[15)] this type of plot can be used to determine the non-recrystallization temperature, T_{nr}.[16)] The change in slope defines this temperature, although there is some ambiguity, because the MFS *vs.* $1/T$ relation is not exactly linear. As expected, the reference alloy has the lowest T_{nr}-value of 877°C and the addition of Nb raises T_{nr}. The lowC–Mn–Nb steel, in which most of the Nb is in solid so-

lution due to the low C and N content, has a T_{nr} value of 920°C. This value is lower than the T_{nr} of the 0.02w%C–Nb steels with a similar Nb-content. In these steels, Nb is supposed to be bonded to C and/or N. The fact that both the C–Mn–Nb and the C–Mn–Nb–N steels have equal T_{nr} temperatures of 950°C, shows that the effect of extra N on T_{nr} is negligible.

Although T_{nr} is a very important temperature in industrial hot rolling mills and the multideformation testing method is universally accepted as testing procedure for the laboratory determination of T_{nr}, the temperature value on itself does not provide a lot of fundamental information on the recrystallization–precipitation interaction. From that point of view, testing methods that can characterize the recrystallization behavior during the complete time interval between two deformation passes, could be a lot more useful. Therefore, the isothermal recrystallization behavior was studied with double deformation tests.

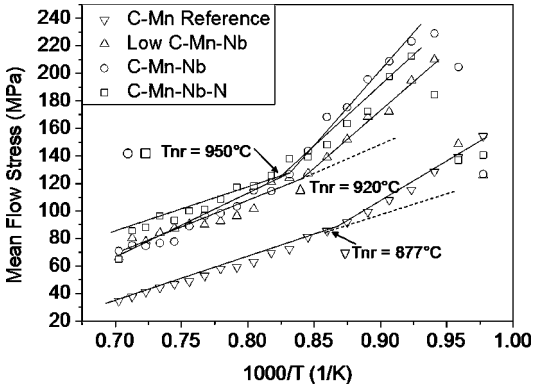

Fig. 1. Mean flow stress *vs.* the inverse of absolute temperature and T_{nr} determination for the four experimental steels.

3.2. Characterization of the Isothermal Recrystallization Behavior

The isothermal recrystallization kinetics were studied by means of double-hit compression tests with variable interpass times. The recrystallized fraction was determined with the help of the second stress–strain curve. If the interpass time is sufficiently long enough for full softening to occur, the second flow curve should be identical to the first flow curve. If there is no softening at all, the second flow curve should appear as an extrapolation of the first flow curve. In order to quantify the amount of softening between these extremes, the 2% offset method was used. With that method the softening effects by recovery can be neglected[17,18] and consequently the calculated softening fraction is linearly related to the statically recrystallized volume fraction. Double-hit compression tests were performed with the four experimental alloys, using deformation temperatures between 850 and 1 075°C and interpass times between 1 and 5 000 s. The results of the softening analysis are shown in **Fig. 2** while the microstructural verification of the recrystallization process is discussed in the next section.

From Fig. 2(a), it is evident that the reference alloy has the fastest recrystallization kinetics and recrystallizes fully at all testing temperatures. At temperatures of 950 and 1 000°C, the recrystallization starts 1 s after the first deformation and is completed in about 100 s. At lower temperatures, 900°C and 850°C, the recrystallization is retarded and starts about 10 and 50 s after the first deformation pass, respectively. In this case, the material is fully recrystallized after 200 and 1 000 s, respectively. It should be noted that the multideformation torsion tests described earlier, revealed a T_{nr} of 877°C for this steel composition. The interpass time during the torsion tests was 20 s; accordingly, one would expect that the material would be fully recrystallized in 20 s at temperatures higher than 877°C. The results from Fig. 2(a) show that at 900°C and 20 s interpass time the recrystallized fraction is only 27%. This apparent contradiction can be explained based on the difference in grain size

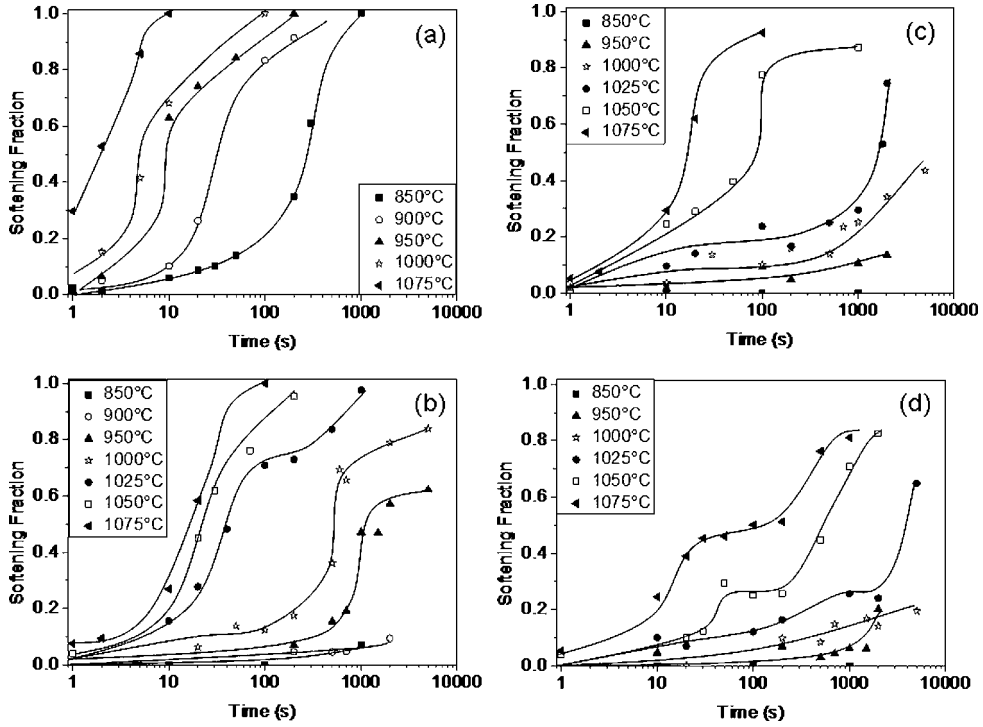

Fig. 2. Softening fractions for the experimental steels determined from double deformation tests, (a) C–Mn reference, (b) lowC–Mn–Nb, (c) C–Mn–Nb and (d) C–Mn–Nb–N.

at a deformation temperature of 900°C. At this temperature, the torsion test sample has already undergone a large number of deformation passes and accumulated a large amount of total deformation. This thermomechanical treatment should have lead to a distinct degree of grain refinement in the austenite by repeated recrystallization cycles. Alternatively, the grain size in the double-hit compression sample just before the first deformation step is expected to be relatively large due to the high reheating time and temperature, *i.e.* 300 s at 1 250°C for both tests, and the lack of deformation prior to the double-hit test. As the grain size is reduced in the torsion samples, the recrystallization kinetics are supposed to be faster and thus the T_{nr} temperature, determined by the multideformation torsion tests, is expected to be lower.[18)]

The other alloys clearly show retarded recrystallization kinetics in comparison with the C–Mn reference alloy which is in agreement with the values of T_{nr} temperatures mentioned above. The T_{nr} temperatures of the Nb-added steels were also higher than the T_{nr} from the reference alloy. The double deformation tests seem to reveal a temporary or even permanent recrystallization stop. The times and temperatures at which this plateau appears can be linked to the precipitation state of the material and will be discussed below. The differences between the lowC–Mn–Nb from Fig. 2(b) and C–Mn–Nb alloy from Fig. 2(c) were rather small. There was good agreement for the highest temperatures, *i.e.* 1 075 and 1 050°C, as well as for the lowest temperature, *i.e.* 850°C: At the highest temperatures both alloys were fully recrystallized within 100 s, and at the lowest temperature no recrystallization was observed, even after 1 000 s. For the intermediate temperatures of 950, 1 000 and 1 025°C some small differences in recrystallization behavior appeared. While at 1 025°C, for the lowC–Mn–Nb alloy, recrystallization started after 10 s and completed after 1 000 s, the C–Mn–Nb alloy only showed a fraction of 30% recrystallization after an interpass time of 1 000 s at this temperature. The differences at these intermediate temperatures indicated that the Nb as a precipitate in C–Mn–Nb alloy had a slightly stronger retarding effect on the recrystallization kinetics than the Nb in solid solution in the lowC–Mn–Nb alloy. This confirms the result of the multideformation torsion tests: Nb as a precipitate, *cf.* C–Mn–Nb alloy, is more effective for retarding the recrystallization than Nb in solid solution, *cf.* the lowC–Mn–Nb alloy.

The differences in recrystallization kinetics between the C–Mn–Nb alloy from Fig. 2(c) and the C–Mn–Nb–N alloy from Fig. 2(d) were not expected since both steels have equal T_{nr} temperatures of 950°C. At temperatures between 850°C and 1 025°C the materials show similar behavior, but at 1 050°C and 1 075°C the C–Mn–Nb alloy recrystallizes much faster. At those high temperatures a plateau is present in the C–Mn–Nb–N alloy while the C–Mn–Nb alloy follows the typical Avrami-relationship and recrystallizes fully within 100 s. Again, precipitates have a considerable influence on the observed differences as will be discussed below.

3.3. Microstructural Evolution

Since the austenite recrystallization is influenced by the austenitic grain size and by the carbide and nitride precipitation, the microstructure as well as the precipitation state prior to deformation were investigated. As shown in **Table 2**, the grain size of the C–Mn reference steel and the lowC–Mn–Nb steel is relatively coarse after the solution treatment at 1 250°C, while the C–Mn–Nb and the C–Mn–Nb–N steels have smaller grains. The smallest austenitic grain size is observed in the C–Mn–Nb–N alloy where also the finest precipitates are present, as was determined on carbon extraction replicas. The latter is in full agreement with the results of Fernandez *et al.*[19)] who ascribe the differences in austenite grain size to the differences in Ti/N ratio. A grain size of 152 μm was found in the C–Mn–Nb steel with a hyperstoichiometric Ti/N ratio, *i.e.* Ti/N=4. A significant smaller grain size of 79 μm was found in the C–Mn–Nb–N steel in which the Ti/N ratio was only 0.7 and thus hypostoichiometric. This, together with the lower Ti supersaturation level in those hypostoichiometric Ti/N steels, leads to an increased tendency to form smaller particles. These small particles are much more effective in pinning the grain boundaries.[20)]

Table 2. Austenite grain sizes and precipitate size prior to deformation.

	Reheating conditions	Austenitic grain size (μm)	Precipitate size (nm)	Precipitate type
C-Mn reference	1250°C – 300s	343	-	-
lowC-Mn-Nb	1250°C – 300s	261	-	-
C-Mn-Nb	1250°C – 300s	152	40 - 80	TiN, (Ti,Nb)(C,N)
C-Mn-Nb-N	1250°C – 300s	79	40 - 80	TiN, (Ti,Nb)(C,N)

The microstructural changes occurring during deformation and subsequent interpass times were evaluated in the quenched dilatometer samples. In **Fig. 3**(a), the microstructure of the lowC–Mn–Nb steel after reheating but before deformation is presented. The grains are large due to grain growth during reheating. Due to the low C and N content in this steel, all carbides and nitrides were dissolved at the used reheating times and temperatures. As a consequence grain growth was not inhibited and the grains obtained a mean size of 261 μm. Figure 3(b) shows the microstructure immediately after the first deformation. The recrystallization will start at the austenite grain boundaries as indicated by the fact that these boundaries are highly serrated. Figure 3(c) confirms that the recrystallized grains nucleated predominantly at austenite grain boundaries, since near the former austenite grain boundary new small grains are visible. This figure corresponds to a fractional softening of 30% as was calculated from the double deformation test (*cf.* Fig. 2(b)). Finally, after long interpass-times, the material is fully softened, see Fig. 3(d). The deformed+100% recrystallized grains with a mean size of 125 μm are remarkably smaller than the original grains before deformation.

4. Characterization of the Precipitation State

The recrystallization behavior is strongly influenced by the precipitation state of the material and thus indirectly by the chemical composition. In this section, the precipitation state of the four alloys is discussed by studying at first the equilibrium precipitation state calculated with Thermocalc and secondly by experimental data on the real precipitation state, *i.e.* weight fraction precipitated and morphology of the precipitates, and on the solute drag effect.

4.1. Precipitation under Thermodynamical Equilibrium Conditions

The Thermocalc software was used to study the precipitation state under equilibrium conditions. For this approach, which was already used by Zou and Kirkaldy,[11)] it was

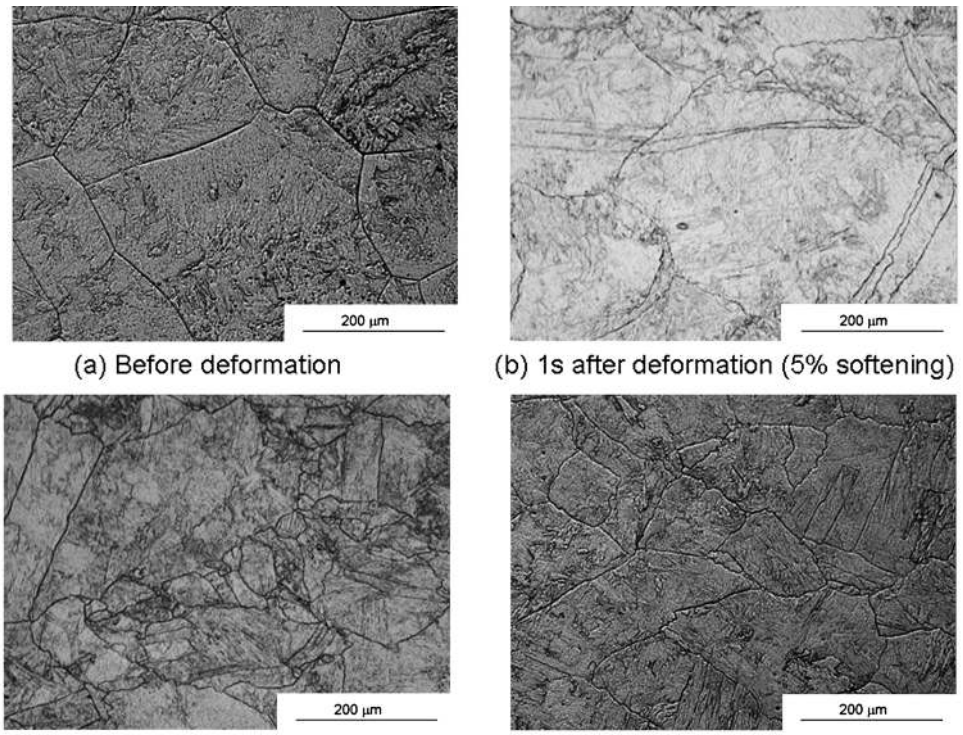

Fig. 3. Austenite recrystallization behavior of microalloyed steels (lowC–Mn–Nb) before deformation and during isothermal holding after first compression (ε=0.2, $d\varepsilon/dt$=0.5/s) at 1 075°C (etching with the Béchet–Beaujard reagent).

assumed that in the austenitic phase, *i.e.* the fcc#1 phase, there was only one type of precipitate. This precipitate has a fcc-structure and is indicated as the fcc#2 phase. This phase contains the elements Ti, Nb, C and N as (TiNb)(CN) in a stoichiometry which varies with temperature. The results from this approximation are presented in **Fig. 4**. This figure shows that in the reference alloy, the precipitate starts forming at 1 250°C and consists mainly of Ti and N. This precipitate is rare, *i.e.* the maximum weight fraction in austenite is 2×10^{-5} wt%, and probably coarse since no strain induced plateau was found in the recrystallization curves from Fig. 2(a). Another possibility why this plateau was not found, is that the precipitates did not completely dissolve during reheating. The reheating temperature for the double deformation tests was 1 250°C and this temperature equals the solubility temperature of the TiN precipitate. In that case the TiN precipitates are coarse and do not have a retarding effect on the austenite recrystallization. For the lowC–Mn–Nb alloy, the precipitate formed at high temperatures (solubility temperature=1 150°C) consists also only of Ti and N. Thermodynamical simulations of the precipitation state of this steel could thus not explain the plateau in the recrystallization–time curve at temperatures between 1 025°C and 900°C. At those temperatures the TiN is expected to be coarse since it has formed at 1 150°C. In the C–Mn–Nb steel again Ti and N containing precipitates are formed at high temperatures. At 1 050°C the mass fraction of the fcc#2 increases significantly and the composition of the precipitate changes completely to Nb and C only. This change/increase should probably be interpreted as a second generation of NbC precipitates nucleating apart from the already existing TiN particles as Liu[12] showed in his work by considering a TiN fcc#2 phase and a NbC fcc#3 phase separately. These newly nucleated and thus small NbC particles are very effective in pinning the grain boundary during recrystallization. A delay in recrystallization could be seen in Fig. 2(c) at temperatures below 1 050°C, *i.e.* the nucleation temperature for NbC precipitates (*cf.* Fig. 4(c)). Also in the C–Mn–Nb–N alloy the stoichiometry of the precipitate varies with temperature, but in a different way than in the C–Mn–Nb alloy. In the C–Mn–Nb–N alloy, there is a temperature range where the precipitate consists mainly of Nb and N. The presence of this NbN dominated precipitates could explain the plateau in the curves at 1 075°C and at 1 050°C, see Fig. 2(d). This plateau was not present in the C–Mn–Nb alloy. At temperatures of 1 025°C and below, the stoichiometry becomes NbC and the recrystallization behavior becomes similar to that of the C–Mn–Nb alloy. The exact stoichiometries of the precipitates will be discussed below.

4.2. Experimental Verification of the Precipitated Weight Fraction

To verify the results from the thermodynamic calculations, the precipitated weight fraction of Nb was determined experimentally by ICP-MS at times corresponding to a softening fraction of 50%, *i.e.* the $t_{0.5}$. This $t_{0.5}$ was directly derived from the experimental results of Fig. 2 and the numerical values for the different materials at different deformation temperatures can be found in **Table 3**. The Nb precipitated weight fraction corresponding to this $t_{0.5}$ as well as the precipitated Nb fraction, which was determined for the main samples, after reheating are also shown in this table. From the double deformation tests and the equilibrium calculations, one would expect that below the solubility temperature, a certain precipitated fraction is found. This fraction is found to increase with a decreasing deformation temperature.

After reheating, see Table 3, a small amount of Nb is precipitated (0.01 wt%) in the C–Mn–Nb and in the

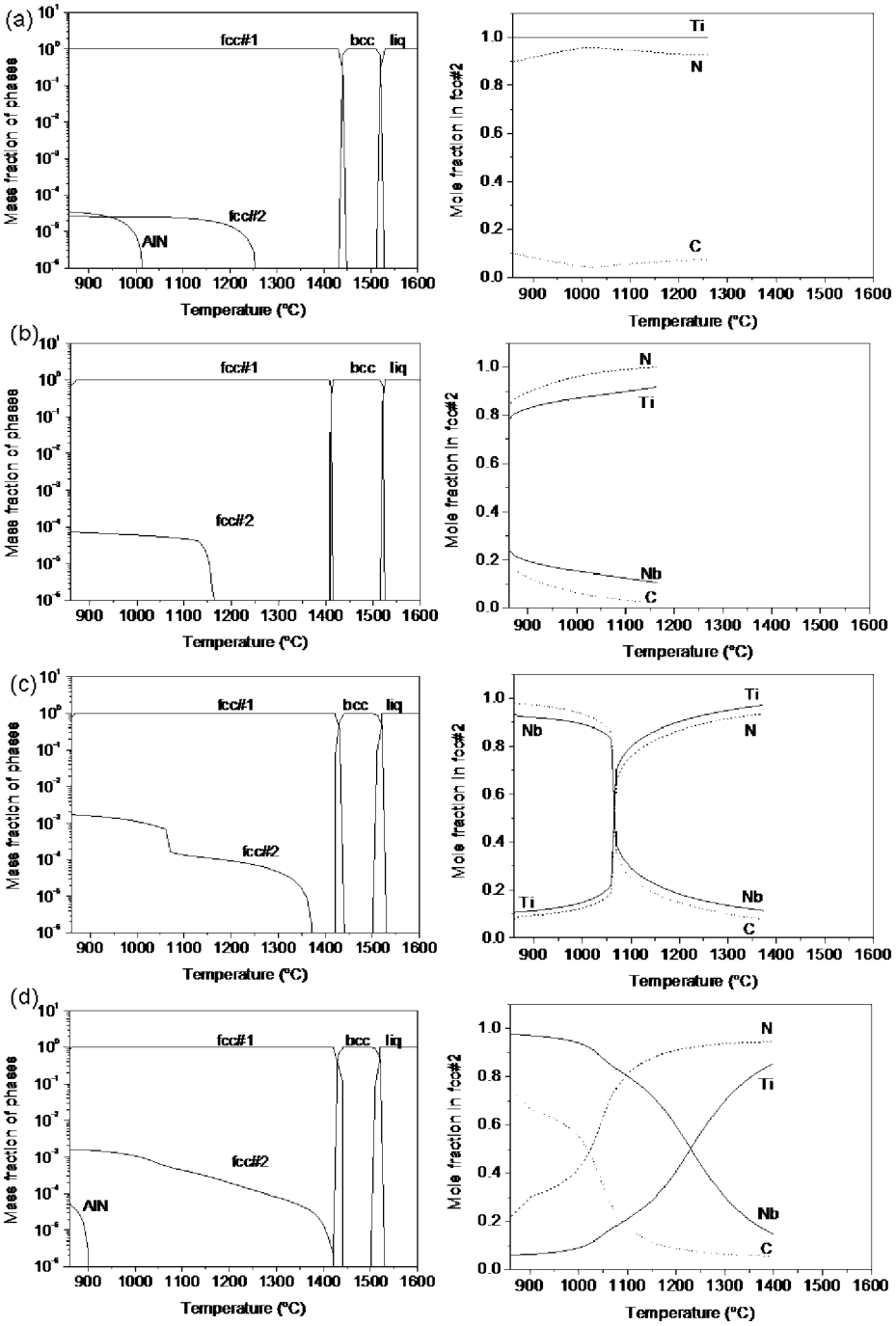

Fig. 4. Phase fraction and fcc#2 compositions of the four experimental steels (Thermocalc), (a) C–Mn reference, (b) lowC–Mn–Nb, (c) C–Mn–Nb and (d) C–Mn–Nb–N.

C–Mn–Nb–N steel. This is in agreement with the results from TEM measurements where (Ti, Nb)(C, N) particles were found after reheating. At deformation temperatures of 1 075°C almost no extra Nb had precipitated in these alloys. For the C–Mn–Nb alloy, this is in agreement with the results from the thermodynamical equilibrium calculations (*cf.* Fig. 4(c)) and with the shape of the recrystallization curve (*cf.* Fig. 2(c)). On the other hand, in the C–Mn–Nb–N alloy, where a clear plateau in the recrystallization curve is visible and where NbN particles were expected according to the equilibrium calculations, only a small amount of extra Nb was precipitated. The amount precipitated is 0.015 wt% at 1 075°C in comparison with 0.01 wt% after reheating. It is possible that this small amount of precipitates is sufficient to cause the temporary recrystallization

Table 3. Precipitated mass fraction of Nb as experimentally determined by ICP-MS. (The mass fractions are determined at times and temperatures corresponding to the $t_{0.5}$).

	lowC-Mn-Nb	C-Mn-Nb	C-Mn-Nb-N
After reheating	-	Nb_{prec} = 0.01wt%	Nb_{prec} = 0.01wt%
T_{def} = 1075°C	$t_{0.5}$ = 17s -	$t_{0.5}$ = 18s Nb_{prec} = 0.013 wt%	$t_{0.5}$ = 200s Nb_{prec} = 0.015 wt%
T_{def} = 1050°C	$t_{0.5}$ = 22s Nb_{prec} = 0.012 wt%	$t_{0.5}$ = 63s Nb_{prec} = 0.02 wt%	$t_{0.5}$ = 500s Nb_{prec} = 0.04 wt%
T_{def} = 1025°C	$t_{0.5}$ = 40s Nb_{prec} = 0.016 wt%	$t_{0.5}$ = 1400s Nb_{prec} = 0.04 wt%	$t_{0.5}$ = 4000s -
T_{def} = 1000°C	$t_{0.5}$ = 580s Nb_{prec} = 0.03 wt%	$t_{0.5}$ = 7000s Nb_{prec} = 0.06 wt%	$t_{0.5}$ = 10000s -
T_{def} = 950°C	$t_{0.5}$ = 1300s Nb_{prec} = 0.03 wt%	$t_{0.5}$ > 10000s -	$t_{0.5}$ > 10000s -

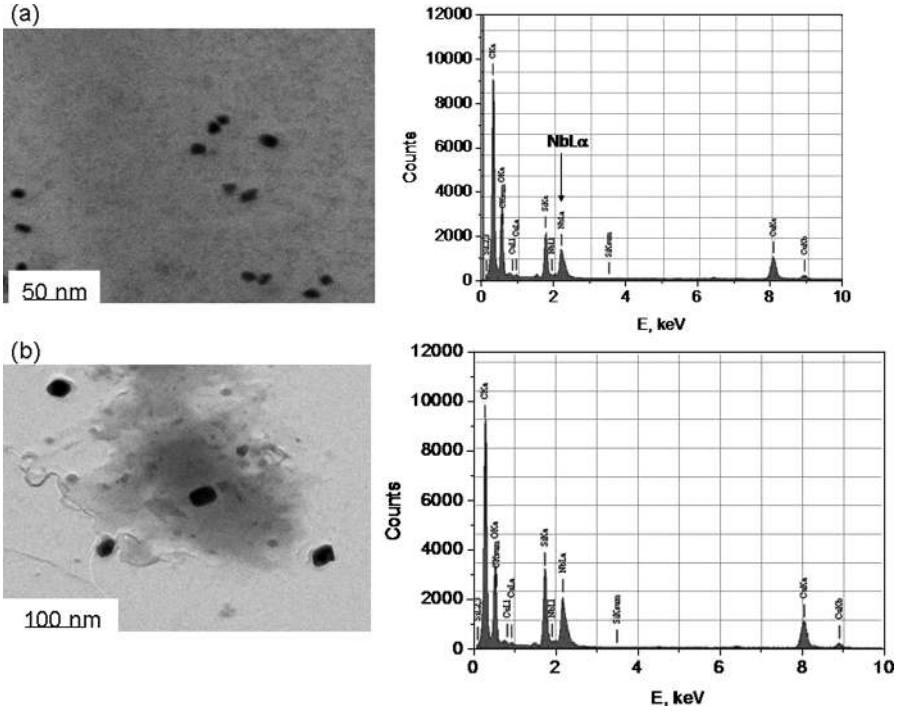

Fig. 5. TEM-EDX measurements on extraction replicas show the presence of small NbC precipitates in the lowC–Mn–Nb alloy after double deformation. (a) T_{def}=1 000°C, interpass-time=580 s, (b) T_{def}=950°C, interpass-time=1300 s.

stop but it is also possible that the precipitated fraction measured on the ICP-MS filter underestimates the true precipitated fraction if small precipitates have passed through the filter and were thus not measured. At 1 050°C, no extra precipitates were observed in the lowC–Mn–Nb alloy, while the amount of Nb precipitated increased to 0.02 wt% and even to 0.04 wt% in the C–Mn–Nb alloy and in the C–Mn–Nb–N alloy, respectively. This higher fraction of Nb precipitated causes an extra increase in $t_{0.5}$. The stoichiometry of the precipitates responsible for the delay will be discussed in the next section. At 1 000°C also in the lowC–Mn–Nb alloy a precipitated weight fraction of 0.03 wt% was found. With TEM it was proven that these precipitates, which were found to be NbC precipitates, are rather small. Their mean size at 1 000°C was 15 nm while they had grown to 40 nm at 950°C, see **Fig. 5**. These precipitates were not expected based on the Thermocalc simulations, although its actual presence could explain the delay in the recrystallization curve at 1 000°C. Moreover, it seems to be unlikely to precipitate out 0.03 wt% of Nb as NbC since this steel contains only 0.0011 wt% of C, leading to a maximum fraction of 0.0085 wt% of Nb precipitated. A possible explanation for this discrepancy could be the presence of other Nb containing precipitates, such as Nb_2C, Fe_2Nb or even Fe_3Nb_3C. These precipitates were regularly found in ferritic stainless steels[21,22] with Nb/C ratios of at least 30/1, but were never reported in microalloyed steels, *i.e.* steels in which the Nb/C ratio is usually smaller than the stoichiometric ratio of 8/1. The Nb/C in the lowC–Mn–Nb steel used in this work is 145/1, so it is not unthinkable that Nb-precipitates, other than the stoichiometric NbC, had been formed. The exact stoichiometry of the precipitates in those steels is studied more in detail in the next section.

4.3. Stoichiometry of the Precipitates Measured by XRD

The results of the experimentally determined weight fractions demonstrated some differences between the precipitation state of the C–Mn–Nb and the C–Mn–Nb–N alloy. At a temperature of 1 050°C, the amount of Nb precipitated in the C–Mn–Nb–N alloy was remarkably higher than the amount of Nb precipitated in the C–Mn–Nb alloy. Thermodynamic equilibrium calculations ascribed the higher fraction of Nb precipitated in the C–Mn–Nb–N alloy to the formation of NbN and/or NbCN. To prove the existence of the NbN, the stoichiometry of the present precipitates is determined. So far, researchers determined the stoichiometry of the complex (Nb, Ti)(C, N) precipitates mainly with TEM, using EDX measurements on thin foils or by indexing diffraction patterns[23] on carbon extraction replicas. More recently, Craven *et al.*[13] described also the use of Parallel Electron Energy Loss Spectroscopy (PEELS) to determine the stoechiometry of precipitates. A PEELS spectrum from a precipitate in a microalloyed steel is compared to PEELS spectra taken from samples of commercial NbC and NbN powders. By using the spectrum from NbN powder as a background under the C K-edge, the C content of the precipitate can be compared with the C content in the NbC powder to calculate the exact fraction of C in the precipitate. In this work, an alternative route is used to determine the stoichiometry of the precipitates. The method uses X-ray diffraction on the filters, obtained from the selective dissolution, and has thus the advantage that the often time consuming and complicated thin foil preparation can be avoided or that also the C-stoichiometry can be determined, which is not the case for C-replicas. From the positions of the peaks in the intensity *vs.* 2θ spectrum, the lattice parameter, and thus the stoichiometry of the present precipitates could be determined. The method of measuring the filter, which only contains precipitates and not the as de-

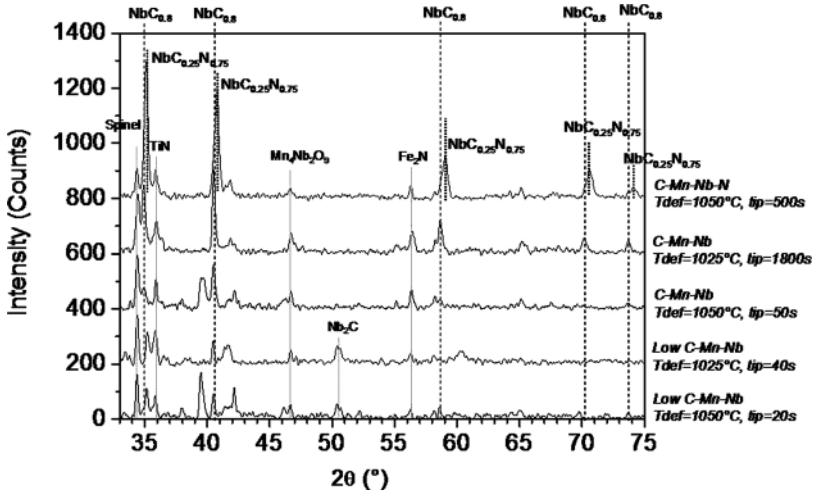

Fig. 6. Determination of the stoichiometry of the precipitates in three of the experimental steels by XRD measurements on ICP-MS filters. The filters were prepared from the quenched samples after double deformation. The deformation temperatures and interpass times are indicated on the graph.

formed material in a whole, *i.e.* precipitates and matrix, has the advantage that the peaks due to precipitation cannot overlap with matrix peaks and/or do not disappear in the background of the matrix. Five filters were measured and the results are presented in **Fig. 6**. A few complex precipitates are present on all five the filters. Further, evidence of $NbC_{0.8}$ (cubic) precipitates with a lattice parameter of 0.445 nm was found in the C–Mn–Nb alloy, while in the lowC–Mn–Nb alloy, at the measured temperatures these precipitates were absent. Some other peaks were found in the lowC–Mn–Nb alloy only, *i.e.* the peak found at 50.3°. This peak was identified as hexagonal Nb_2C and leads to a maximum fraction of Nb precipitated of 0.017 wt%, which nicely agrees with the experimentally determined fraction of 0.016 wt% of Nb precipitated at 1 025°C. However, the presence of Nb_2C only, cannot explain the experimentally determined amount of 0.03 wt% of Nb precipitated at 1 000°C and at 950°C. It is possible that at those lower temperatures also other Nb-containing precipitates are present, such as Fe_2Nb and Fe_3Nb_3C.[21,22] Due to a lack of thermodynamic data on these precipitates, it is at present not possible to accurately determine their solubility temperatures indicating their presence at 1 000 and 950°C. However, the plateau that strongly delays the recrystallization at 1 000 and 950°C, see Fig. 2(b), as well as the presence of Nb_2C at higher temperatures, argue in favour of the existence of hyperstoichiometric Nb/C precipitates and thus tends to confirm the experimentally determined weight fraction of 0.03 wt%.

In the C–Mn–Nb–N alloy the same peaks as in the C–Mn–Nb steel, *i.e.* $NbC_{0.8}$ peaks, were found, although a little bit shifted towards higher angles when compared to the peaks in the C–Mn–Nb steel. This shift corresponds to a somewhat lower lattice parameter of 0.441 nm indicating the presence of more nitrogen in the precipitates. Knowing this lattice parameter, the C and N content in the precipitate could be determined according to Vegard's law.[24] According to this law, the lattice constant of a NbCN complex compound is expressed by Eq. (1) based on the assumption of Eq. (2):

$$a_{NbCN} = a_{NbN} \cdot y_N + a_{NbC} \cdot y_C \quad \text{.....(1)}$$

$$y_C + y_N = 1 \quad \text{.....(2)}$$

In which y_C and y_N represent the fraction of C and N in the sublattice of the precipitate according to the two-sublattice model.[25] The values of the lattice constants of NbC and NbN are taken from the work of Inoue *et al.*[10] In that way, a stoichiometry of $NbC_{0.25}N_{0.75}$ was found from the X-ray spectrum. The found stoichiometries of the precipitates are in good agreement with the stoichiometries calculated under equilibrium conditions. This confirms the statement of Pandit *et al.*[26] who declared that deformation will greatly enhance the kinetics of precipitation but that the nature and the chemical composition of the precipitates is expected to remain the same as in the situation without deformation.

4.4. Quantification of the Solute Drag Effect

Equilibrium calculations as well as the experimentally determined precipitated weight fraction showed that for all the steels in this work, the maximum amount of Nb precipitated is rather low. The low amounts precipitated (maximum 0.06 wt% Nb) compared to the high total amount of 0.16 wt% Nb in the steel, means that a rather high amount of Nb is still present in solution. This Nb in solution will cause an extra delay on the nucleation and growth stages of the recrystallization process. The retardation in the nucleation stage of the recrystallization is due to inhibition of dislocation climb, while the retardation in the growth stage is due to interference of the segregated Nb atom with the recrystallizing grain boundaries.

To quantify this solute drag effect it is necessary to define $\tau_{0.5}$, the normalized time to induce 50% softening, which is the real time to induce 50% softening, $t_{0.5}$, corrected by a grain size and a strain effect. Sellars[2] proposed the following relationship for $t_{0.5}$ in C–Mn–Nb steels:

$$t_{0.5} = C \cdot d_0^2 \cdot \varepsilon^{-4} \cdot \exp\left(\frac{Q_{rex}}{RT}\right) \quad \text{.....(3)}$$

In which d_0 is the former austenitic grain size, ε the true strain, Q_{rex} the activation energy for static recrystallization, T the temperature, C a constant and R the universal gas constant. The normalized time to induce 50% softening is then:

$$\tau_{0.5} = t_{0.5} \cdot d_0^{-2} \cdot \varepsilon^4 = C \cdot \exp\left(\frac{Q_{rex}}{RT}\right) \quad \text{.....(4)}$$

This $\tau_{0.5}$ is only function of temperature for a specific steel. Thus from Eq. (4), the normalized time can be determined if d_0, $t_{0.5}$ and e are known. In this work, d_0 and $t_{0.5}$ were determined experimentally, see Table 2 and Table 3, respectively; the value of ε was 0.2. It is usually found that the effect of solutes on $\tau_{0.5}$ follows an exponential law.[27,28] In the present case, it is:

$$\tau_{0.5}=A\cdot\exp(\mathrm{SRP}_{0.5}\cdot[\mathrm{Nb}]_{\mathrm{sol}}) \quad \text{.....(5)}$$

Where A is an experimental constant, $[\mathrm{Nb}]_{\mathrm{sol}}$ the concentration of Nb in solution in weight percent and a solute retardation parameter ($\mathrm{SRP}_{0.5}$) which can be used to quantify the solute effect at 50% of softening. The value of $\mathrm{SRP}_{0.5}$ can be determined by comparing $\tau_{0.5}$ of the C–Mn–Nb alloy at 1 075°C with $\tau_{0.5}$ of the C–Mn reference alloy at 1 075°C. At that temperature there is no evidence for precipitation in the C–Mn–Nb steel and the delay on $t_{0.5}$ is solely due to solute drag. To calculate $\mathrm{SRP}_{0.5}$ in that situation, Eq. (5) can be approximated as[29]:

$$\mathrm{SRP}_{0.5}=\frac{d\ln\tau_{0.5}}{d[\mathrm{Nb}]_{\mathrm{sol}}}\approx\frac{\ln(\tau^1_{0.5}/\tau^2_{0.5})}{[\mathrm{Nb}]^1_{\mathrm{sol}}-[\mathrm{Nb}]^2_{\mathrm{sol}}} \quad \text{.....(6)}$$

In which $\tau^1_{0.5}$ is the normalized $t_{0.5}$ for the C–Mn–Nb alloy at 1 075°C and $\tau^2_{0.5}$ the normalized $t_{0.5}$ for the reference alloy at 1 075°C. Similarly $[\mathrm{Nb}]^1_{\mathrm{sol}}$ and $[\mathrm{Nb}]^2_{\mathrm{sol}}$ are the solute Nb concentration at 1 075°C in the C–Mn–Nb alloy (0.16 wt%, see Table 3) and in the reference alloy (0 wt%), respectively. Substituting the $\tau_{0.5}$ into Eq. (6) and normalizing the solute Nb concentrations to 0.1 wt%, $\mathrm{SRP}_{0.5}$ was calculated to be about 239. This value is in close agreement with the value of 222 for Nb at 50% softening as reported by Jonas.[30] To determine whether the solute drag effect of Nb is stronger in the nucleation stage or in the growth stage of the recrystallization process, the solute retardation parameter at 5% softening, $\mathrm{SRP}_{0.05}$, was also calculated. Therefore, in Eq. (6) $\tau^1_{0.5}$ and $\tau^2_{0.5}$ were replaced by $\tau^1_{0.05}$ and $\tau^2_{0.05}$ respectively. $\tau^1_{0.05}$ is the normalized time at 5% softening for the C–Mn–Nb alloy at 1 075°C and $\tau^2_{0.05}$ the normalized time at 5% softening for the C–Mn reference alloy at 1 075°C. The solute retardation parameter at 5% softening was found to be 177. This value is remarkably smaller than the value of 239 found at 50% softening, indicating that Nb in solution mainly delays the migration of grain boundaries, *i.e.* the grain growth stage, and to a lesser extent the formation of new dislocation free nuclei, *i.e.* the nucleation stage of the recrystallization process.

With the calculated value of $\mathrm{SRP}_{0.5}$, the ratio between the time for 50% softening due to solute drag of Nb in the C–Mn–Nb steel and the time for 50% softening in the reference steel was calculated at lower temperatures. This ratio was found to vary between 8 and 8.8 in the temperature range from 1 075 to 1 000°C. For the solute drag effect of Nb in the lowC–Mn–Nb alloy, comparable ratios between 8.7 and 9 were found. The limited differences between those ratios make it possible to construct the dashed line in **Fig. 7** as a parallel to the $t_{0.5}$ line of the C–Mn reference steel. This dashed line represents the retardation on the recrystallization due to solute drag of Nb in solution. This so called "Nb solute drag line" allows us to quantify the magnitude of the solute drag and the precipitation effect directly from a softening-time-temperature diagram.

The C–Mn–Nb–N steel deviates from the Nb solute drag line at all temperatures tested in this work. It is concluded that the retardation of the recrystallization behavior in this steel at all temperatures is caused by a combination of

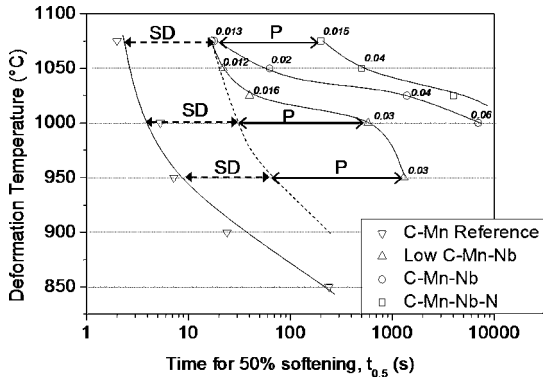

Fig. 7. Softening–time–temperature diagrams for the four experimental steels. (Plotted is the time for 50% softening and the corresponding weight fraction of precipitated Nb (in italics), see also Table 3; SD=solute drag, P=precipitation).

solute drag and precipitation. In Fig. 7, the former is indicated as SD and the latter as P. While on a logarithmic scale the magnitude of the solute drag effect is almost constant over the temperature range, the magnitude of the precipitation effect seems to increase with decreasing temperatures. Equilibrium calculations as well as XRD measurements showed that, at 1 075°C and at 1 050°C, NbN precipitates are responsible for the delay, while at 1 025°C it is mainly NbC. The fact that at 1 025°C the $t_{0.5}$ curve of the C–Mn–Nb–N steel approaches the $t_{0.5}$ curve of the C–Mn–Nb steel, where there are only NbC precipitated, confirms this. The C–Mn–Nb steel starts to deviate from the Nb solute drag line at temperatures of 1 050°C. ICP-MS measurements verified that there was already a small amount of Nb precipitated at that temperature which is probably insufficient to cause a plateau in the softening curve. In the lowC–Mn–Nb steel, the deviation from the Nb solute drag line starts at 1 025°C which is agreement with the plateau observed in Fig. 2(b). Furthermore, it can be noticed that in this alloy, at 1 000°C the main part of the delay on $t_{0.5}$ is caused by a precipitation effect. TEM measurements already confirmed the presence of small NbC precipitates at 1 000°C, see Fig. 5(a). At 950°C, the precipitation effect appears to become smaller again. According to the ICP-MS measurements no extra precipitates had been formed by lowering the temperature from 1 000 to 950°C. The amount of $\mathrm{Nb}_{\mathrm{prec}}$ stays 0.03 wt% which is in agreement with the equilibrium value at that temperatures. TEM measurements at 950°C show that the precipitates had grown at the expense of certain other precipitates that had been dissolved. The average particle size at 950°C is 40 nm, see Fig. 5(b). From the Zener pinning formula,[31] it can be seen that these larger particles are less effective in pinning boundaries of the recrystallized grains. The Zener pinning force is given by:

$$F_{\mathrm{P}}=\frac{3\cdot\gamma_{\mathrm{GB}}\cdot F_{\mathrm{v}}}{2\cdot r} \quad \text{.....(7)}$$

Where γ_{GB}, F_{v} and r represent the grain boundary energy (usually 0.75 J/m^2 in austenite), the precipitate volume fraction and the average precipitate radius, respectively. An increase of the volume fraction of precipitates increases the total driving pinning force, while coarsening at constant volume fraction decreases the pinning force. For the lowC–Mn–Nb alloy at times of 50% softening, pinning forces of $2.3\cdot10^4$ MPa and $8.4\cdot10^3$ MPa were found for

deformation temperatures of 1 000°C and 950°C, respectively. These pinning forces are compared to the driving forces for recrystallization. When the recovery effect during isothermal holding is neglected, this driving force is equal to the stored energy after deformation[32]:

$$F_R = \frac{1}{2} \cdot \rho \cdot \mu \cdot b^2 \quad \text{.....(8)}$$

In which ρ is the dislocation density after deformation ($\sim 3 \cdot 10^{14}\,\mathrm{m}^{-2}$), μ the shear modulus ($\sim 4 \cdot 10^4\,\mathrm{MPa}$) and b the magnitude of the Burgers vector ($\sim 2.53 \cdot 10^{-10}\,\mathrm{m}$). For the lowC–Mn–Nb steel, F_R is found as $4 \cdot 10^5\,\mathrm{MPa}$. The driving force for recrystallization is thus one order of magnitude higher than the pinning force at 1 000°C and almost 2 orders of magnitude at 950°C at times of 50% softening. This agrees well with the results from Fig. 2(b): at times of 50% softening, *i.e.* 580 s at 1 000°C and 1 300 s at 950°C, no plateau is found or thus the recrystallization rate is different from zero.

Although the precipitate sizes, reported in this work, are almost one order of magnitude larger than the ones Hutchinson[6] assumes for the calculations in his work, the tendency is similar: The dominant mechanism in retarding the austenite recrystallization changes from precipitation, at temperatures just below the solubility temperature, to solute drag, at precipitate coarsening temperatures.

5. Conclusions

In this contribution, the recrystallization behavior was studied extensively by multideformation tests and isothermal double deformation tests and shown to depend strongly on the precipitation state of the material. The results can be summarized as follows:

(1) The addition of 0.17 wt% Nb on the recrystallization behavior was compared by multideformation torsion tests and double hit compression tests. Both testing methods gave consistent results and showed that Nb strongly delays the recrystallization. By adding 0.17 wt% Nb to the reference alloy, T_{nr} was raised by 73°C. With the same amount of Nb but a drastic decrease of C, T_{nr} is raised by only 43°C. This result indicates that Nb as precipitate is more effective in retarding the recrystallization than Nb in solid solution, although it has to be noticed that also in the lowC–Mn–Nb alloy (with only 11 ppm of C) the presence of a small fraction of NbC was found resulting in an extra delay of the recrystallization.

(2) Adding extra N to a C–Mn–0.16wt%Nb steel does not increase T_{nr} but significantly influences the recrystallization behavior in a double deformation test which it delays strongly by the precipitation of fine NbN particles. These NbN particles were not found in the C–Mn–Nb steel with only 20 ppm of N.

(3) Thermodynamic calculations assuming a phase equilibrium between γ and (Nb, Ti)(C, N) were found to give a good approximation for the real precipitation state in a microalloyed steel under deformation conditions. The precipitated fraction as well as the stoichiometry of the precipitates were in good agreement, especially for the C–Mn–Nb and for the C–Mn–Nb–N alloy, with the results from ICP-MS and XRD measurements, respectively. Both experimental results and calculations show that TiN predominantly forms at very high temperatures and that NbC or Nb(C, N) precipitate at lower temperatures.

(4) It was proven that softening–time–temperature diagrams contain a lot of information on the precipitation state of the material. By drawing the solute drag line, the precipitation start temperature is found as the temperature at which $t_{0.5}$ starts to deviate from this solute drag line. By comparing the distance between the $t_{0.5}$ of a reference alloy and the solute drag line with the distance between the solute drag line and the $t_{0.5}$ of a microalloyed steel, a quantification of the solute drag effect and the precipitation effect can be made at all temperatures. Furthermore, the temperature where the precipitation effect becomes again smaller is an indication for the temperature at which precipitate coarsening starts.

REFERENCES

1) T. M. Maccagno, J. J. Jonas, S. Yue, B. J. McCrady, R. Slobodian and D. Deeks: *ISIJ Int.*, **34** (1994), 917.
2) C. M. Sellars: Proc. of Int. Conf. on Hot Working and Forming Processes, ed. by C. M. Sellars and G. J. Davies, Met. Soc., London, (1980), 3.
3) J. G. Speer and S. S. Hansen: *Metall. Trans. A*, **20A** (1989), 25.
4) S. F. Medina, A. Quispe, P. Valles and J. L. Banos: *ISIJ Int.*, **39** (1999), 913.
5) M. J. Luton, R. Dorvel and R. A. Petkovic: *Metall. Trans.*, **11** (1980), 411.
6) C. R. Hutchinson, H. S. Zurob, C. W. Sinclair and Y. J. M. Brechet: *Scr. Mater.*, **59** (2008), 635.
7) R. Coladas, J. Masounave and J. P. Bailon: Proc. Int. Conf. on the Hot Deformation of Austenite, TMS-AIME, New York, (1977), 341.
8) M. G. Akben, I. Weiss and J. J. Jonas: *Acta Metall.*, **29** (1981), 111.
9) H. L. Andrade, M. G. Akben and J. J. Jonas: *Metall. Trans. A*, **14A** (1983), 1967.
10) K. Inoue, N. Ishikawa, I. Ohnuma, H. Ohtani and K. Ishida: *ISIJ Int.*, **41** (2001), 175.
11) H. Zou and J. S. Kirkaldy: *Metall. Trans. A*, **23A** (1992), 651.
12) Z.-K. Liu: *Scr. Mater.*, **50** (2004), 601.
13) A. J. Craven, K. He, L. A. J. Garvies and T. N. Baker: *Acta Mater.*, **48** (2000), 3857.
14) A. Gräber and K. Pöhlandt: *Steel Res.*, **61** (1990), 212.
15) D. Q. Bai, S. Yue, W. P. Sun and J. J. Jonas: *Metall. Trans. A*, **24A** (1993), 2151.
16) M. Gomez, S. F. Medina and P. Valles: Proc. of 2nd Int. Conf. on Thermomechanical Processing of Steels, Liège, Belgium, (2004), 157.
17) A. I. Fernandez, B. Lopez and J. M. Rodriguez-Ibabe: *Scr. Mater.*, **40** (1999), 543.
18) G. Li, T. M. Maccagno, D. Q. Bai and J. J. Jonas: *ISIJ Int.*, **36** (1996), 1479.
19) A. I. Fernandez, P. Uranga, B. Lopez and J. M. Rodriguez-Ibabe: *ISIJ Int.*, **40** (2000), 893.
20) F. B. Pickering: Ttitanium Technology in Microalloyed Steels, ed. by T. N. Baker, The Institute of Materials, London, (1994), 10.
21) G. M. Sim, J. C. Ahn, S. C. Hong, K. J. Lee and K. S. Lee: *Mater. Sci. Eng.*, **396** (2005), 159.
22) V. Kuzucu, M. Aksoy, M. H. Korkut and M. M. Yildirim: *Mater. Sci. Eng.*, **230** (1997), 75.
23) C. Klinkenberg, K. Hulka and W. Bleck: *Steel Res.*, **75** (2004), 744.
24) A. R. Denton and N. W. Ashcroft: *Phys. Rev. A*, **43** (1991), 3161.
25) M. Hillert and L. I. Staffansson: *Acta Chem. Scand.*, **24** (1970), 3618.
26) A. Pandit, A. Murugaiyan, A. Saha Podder, A. Haldar, D. Bhattacharjee, S. Chandra and R. K. Ray: *Scr. Mater.*, **53** (2005), 1309.
27) C. M. Sellars and J. H. Beynon: Proc. Conf. on High Strength Low Alloy Steels, ed. by D. P. Dunne and T. Chandra, ASM, Ohio, USA, (1985), 142.
28) J. C. Herman, P. Messien and T. Gredary: Proc. Conf. on Thermo-Mechanical Processing of Microalloyed Austenite, ed. by A. J. DeArdo, G. A. Ratz and P. J. Wray, AIME, Warrendale, P.A., USA, (1982), 655.
29) W. J. Liu and M. G. Akben: *Can. Metall. Q.*, **26** (1987), 145.
30) J. J. Jonas: Proc. Conf. on High Strength Low Alloy Steels, ed. by D. P. Dunne and T. Chandra, ASM, Ohio, USA, (1984), 80.
31) C. Zener and C. S. Smith: *Trans. Am. Inst. Min. Eng.*, **175** (1948), 15.
32) H. S. Zurob, Y. Brechet and G. Purdy: *Acta Mater.*, **49** (2001), 4183.